Peng Li*

Tribological properties and microstructures of Al_2O_3-TiC-TiB_2 reinforced composites

DOI 10.1515/secm-2015-0055
Received January 22, 2014; accepted January 19, 2016; previously published online April 12, 2016

Abstract: Ti-3Al-2V alloy is an important aviation material but shows poor resistance to slid wear. Laser cladding of the Fe_3Al-B_4C pre-placed powders on a Ti-3Al-2V substrate can form the TiC-TiB_2 reinforced composites, which improved the wear resistance of the substrate. In this study, it was noted that the addition of the Al_2O_3 and 7 wt.% yttria partially stabilized zirconia (YPSZ) was able to further increase the wear resistance of such composites. Al_2O_3 increased the dilution rate of the substrate to the laser molten pool to a certain extent; moreover, Al_2O_3 improved the hardness, elastic modulus and the mechanical properties of such laser clad composites. The YPSZ addition led t-ZrO_2-$ZrSiO_4$ to be produced in such composites.

Keywords: coatings; composites; lasers; wear; zirconia.

1 Introduction

Laser cladding is a useful surface modification technique, because of the following advantages: optimal bond properties, high process flexibility, rapid solidification and no requirement for post-process treatment [1–3]. In recent years, the titanium alloys have been widely used in many fields, but its surface does not have enough wear resistance, limiting their potential applications [4]. Laser cladding of the Fe_3Al-B_4C mixed powders on the Ti-3Al-2V alloy can form composites, which improves greatly the wear resistance of the substrate.

Liang et al. [5] and Jiang et al. [6] reported that recent years have seen the development of TiC-TiB_2 reinforced coatings, which represented promising materials to be used as wear resistance parts and high-temperature structural components. Fe_3Al also has a lot of good performances, such as wear resistance, oxidation resistance, high temperature resistance and corrosion resistance. Laser cladding of the Fe_3Al-B_4C pre-placed powders on the Ti-3Al-2V alloy substrate can form TiC-TiB_2 reinforced Fe_3Al-Ti_3Al matrix composites, which improved greatly the wear resistance of the substrate; nevertheless, during the laser-cladding process, a large amount of TiC-TiB_2 in the molten pool absorbed much energy from the laser beam, thus resulting in decrease of the dilution rate of the substrate to the coating. The yttria partially stabilized zirconia (YPSZ) addition in such coating is an effective way to control the cracks and relatively fine substructure of the laser clad composites [7]. Investigations [8, 9] also indicated that the Al_2O_3-ZrO_2 ceramics on metal substrate are desirable for wear resistance and erosion resistance.

In this study, the effect of YPSZ-Al_2O_3 on the wear resistance and microstructures of the Fe_3Al/B_4C laser clad composites is introduced. This research provides experimental and theoretical experimental basis to promote laser technology in the field of the surface modifications of the metals.

2 Materials and methods

The materials used in this experiment were as follows: Ti-3Al-2V alloy (6 wt.% Al, 4 wt.% V, ≤0.3 wt.% Fe, ≤0.1 wt.% C, ≤0.15 wt.% Si, ≤0.2 wt.% O, balance Ti) samples (10 mm×10 mm×10 mm), and the thickness of the pre-placed layer was 0.6~0.8 mm and was polished with SiC grit paper prior to the coating operation; alloy powders of Fe_3Al (≥99.5% purity, 50~200 μm), B_4C (≥99.5% purity, 50~150 μm), Al_2O_3 (≥98.5% purity, 150~250 μm) and YPSZ (7 wt.% Y_2O_3, 50~100 μm) were used for the laser cladding, and the water glass was used as the joining material. A 1.5 kW continuous wave of CO_2 laser with a beam diameter of 4.5 mm was employed to melt the surface of the samples. Three-track lap coating was formed on the substrate, and the lap rate was approximately 25%. During the laser-cladding process, surface oxidation was prevented by inert gas (Ar) with a flow rate of 35 L/min. Compositions of the pre-placed powders used were 47.5 wt.% Fe_3Al+40 wt.% B_4C+10 wt.% Al_2O_3+2.5 wt.% YPSZ.

The wear volume loss was measured every 10 min. The wear resistance of these laser-cladded ceramic layers was tested by the MM200 (Wuhan Unity Laser Limited Company, Wuhan, P.R. China) disc wear tester (Beijing Western Lofty Technology Limited Company, Beijing, P.R. China). The

***Corresponding author: Peng Li,** Mechanical and Electronic Engineering Department, Shandong Agriculture and Engineering University, Jinan 250100, P.R. China, e-mail: lpalsh@126.com

rotational speed of the wear tester was 465 rpm. The linear velocity of the friction surface was 0.88 m/s.

X-ray diffraction (XRD) (Rigaku Corporation, Osaka, Japan) test equipment was used to determine the phase constituent of such laser clad composites; the microstructure morphologies of such composites was analyzed by means of a scanning electron microscope (SEM) (Leo Germany Electron Limited Company, Ruhrgebiet, Germany); an elements' distributions of such composites were measured using energy dispersive spectrometer (EDS) (Leo Germany Electron Limited Company, Ruhrgebiet, Germany); HV-1000 microsclerometer (Shanghai Zhongyan Instrument Manufacturing Plant, Shanghai, P.R. China) was used to test the micro-hardness distribution of such composites.

3 Results and analysis

3.1 XRD and EDS analysis

As was shown in Figure 1, the surface of the Fe_3Al-B_4C-YPSZ-Al_2O_3 laser clad composites mainly consisted of Fe_3Al, Ti_3Al, TiB_2, TiC, Al_2O_3, TiO_2, t-ZrO_2 and $ZrSiO_4$. It should be mentioned that the Y_2O_3 diffraction was not present in the XRD diagram due to its too low content. As mentioned previously, there was SiO_2 in the water glass. According to the research of Xue et al. [10], it was known that the addition of YPSZ may decrease the intergranular glassy SiO_2 phases by forming $ZrSiO_4$ and hence improve various mechanical properties of such composites [11]. As the stabilizer of ZrO_2, Y^{3+} in Y_2O_3 can suppress c→t→m transformation, and the content of Y^{3+} has a different suppression effect on ZrO_2 transformation, which enables metastable phase tetragonal ZrO_2 (t-ZrO_2) to exist, while t-ZrO_2 phase structure has stress-induced transformation character, which has transformation toughness action [12].

In fact, during the laser-cladding process, Ti were able to enter into the molten pool due to the dilution effect of the substrate to laser molten pool; moreover, Ti and Al were all the activity elements, which were able to react with oxygen in the air leading to the formation of TiO_2 and Al_2O_3, respectively. In addition, a large amount of Al in the molten pool came from the substrate. Thermodynamically, a portion of Al had high affinity with Ti, favoring the formation of Ti_3Al.

It was known that Al_2O_3 was also able to react with a portion of TiB_2 in the molten pool, leading to the formations of Ti_3Al and B, thus resulting in the production of the high Ti_3Al diffraction peak. In addition, with decrease of TiB_2, the dilution rate of the substrate to the coating increased, leading to the complete melting of retained TiB_2. As a result, the fine microstructure was obtained. The XRD diagram also indicated that TiB_2-TiC can be produced through *in situ* metallurgical reactions during the laser-cladding process, the chemical reaction which accorded with thermodynamic laws can take place as follows [13]:

$$3Ti+B_4C \rightarrow 2TiB_2+TiC. \quad (1)$$

The EDS image indicated that there were B, C, O, Al, Ti and Zr in point 1 of the upper layer (see Figure 2A and B). Combining the XRD image indicated that the precipitates of the upper region consisted mainly of t-ZrO_2, TiO_2, TiB_2 and TiC. It was known that the melting points of TiC (3420°C) and TiB_2 (2980°C) were higher than those of TiO_2 (2050°C)-ZrO_2 (2677°C), so it can be deduced that t-ZrO_2/TiO_2 precipitated around TiB_2/TiC. Vasiliev and Padture [14] reported that Al^{3+} was otherwise insoluble in t-ZrO_2 at room

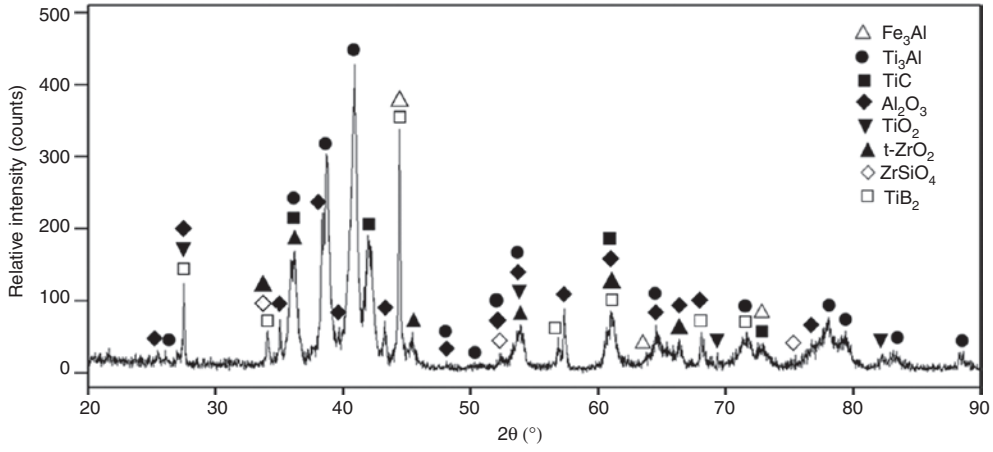

Figure 1: X-ray diffraction diagram of the Fe_3Al-B_4C-YPSZ-Al_2O_3 laser clad composites.

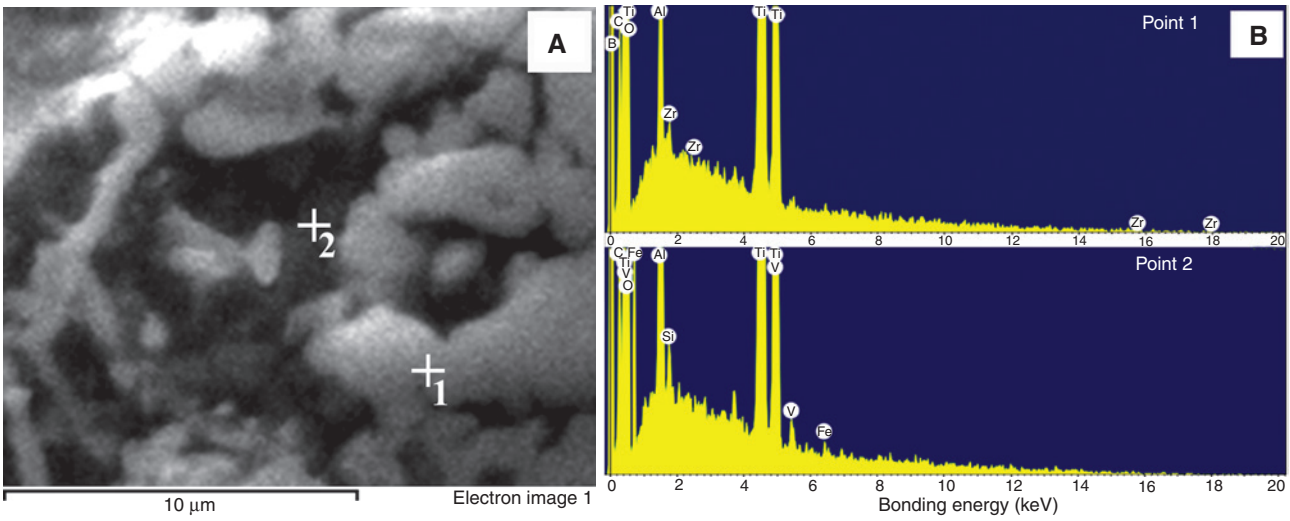

Figure 2: SEM image of the upper layer in the Fe_3Al-B_4C-YPSZ-Al_2O_3 laser clad composites and the EDS spectrum analysis, (A) microstructures and (B) points 1 and 2.

Table 1: EDS results of the different points in the Fe_3Al-B_4C-YPSZ-Al_2O_3 laser clad composites.

Position	Elements (atomic.%)								
	B	C	O	Al	Si	Ti	V	Fe	Zr
Position 1	3.78	14.78	35.59	2.45	–	41.84	–	–	1.56
Position 2	–	24.28	27.90	9.71	0.34	30.60	1.54	5.63	–

temperature under equilibrium conditions and was in solid solution with ZrO_2, leading to the stabilization of t-ZrO_2.

The EDS image of point 2 indicated that there were C, O, Al, Si, Ti, Fe and V in the matrix of the upper layer, and the EDS images of these two different points are shown in Table 1. According to the XRD test result, it can be deduced that there were Fe_3Al, Ti_3Al, Al_2O_3, $ZrSiO_4$ and TiC in the matrix of the upper layer. It was considered that there was a minor amount of inter-dendritic TiC-Fe_3Al eutectic in the matrix of the upper layer. According to Jackson's theory of interface structure, the solid/liquid interface of the TiC carbide is atomically smooth, and its growth mechanisms are predominantly by lateral growth under equilibrium and near-equilibrium solidification conditions [15]. Thus, it was reasonable that the t-ZrO_2-TiB_2-TiC precipitates embedded in the composite matrix; moreover, it should be mentioned that ZrO_2 has an action of transformation to toughening on the Al_2O_3 matrix [16].

3.2 Microstructures analysis

As is shown in Figure 3A, a stratification was observed in such laser clad composites. It was considered that

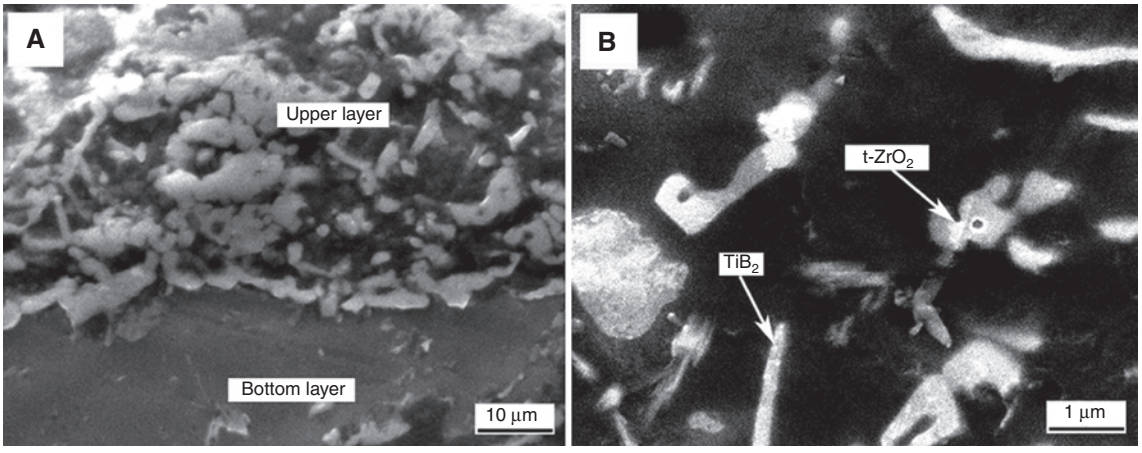

Figure 3: SEM micrographs of the Fe_3Al-B_4C-YPSZ-Al_2O_3 laser clad composites, (A) upper layer and (B) TiB_2 and t-ZrO_2.

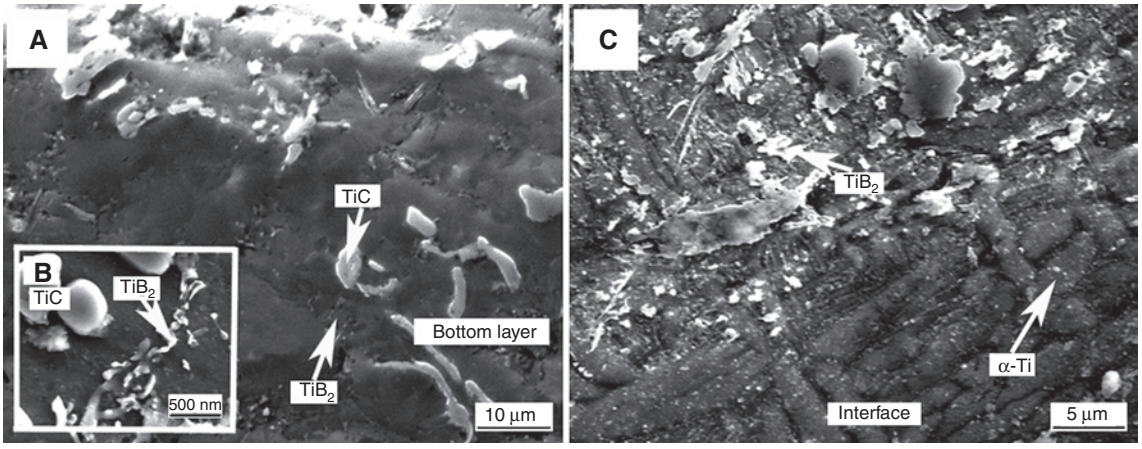

Figure 4: SEM micrographs of the Fe_3Al-B_4C-YPSZ-Al_2O_3 laser clad composites, (A) bottom layer, (B) TiC and the TiB_2 cluster, and (C) the interface zone.

the completed melting of both ceramics and alloy had occurred during the laser radiation, and there was some redistribution of components because of the difference of the mass density and interfacial tension between two liquid phases, boosted by the drastic convection in the molten pool. The clad zone can be divided into three distinct regions: the upper layer, the bottom layer and the transition layer. The upper layer was approximately 250 μm thick, and there was t-ZrO_2 in this region. It was known that the density of YPSZ was 4.15 g/cm^3, which was lower than that of the density of TiB_2 (4.52 g/cm^3) or TiC (4.93 g/cm^3). Thus, it was reasonable that during the laser-cladding process, YPSZ had a very marked trend to float on the top of the molten pool; moreover, the production of TiO_2 reduced the thermal stress and also the solidification shrinkage of such composites, which was beneficial to the controllable cracking in the clad layer. The SEM micrographs of the upper layer were shown in Figure 3B for sections perpendicular to the growth direction. Combining the XRD image, it can be deduced that TiB_2 was produced in this region. The investigation [17] indicated that during the laser-cladding process, TiB_2 precipitated earlier due to the high melting point, which gave nucleation sites for the future grains, favoring the formation of a fine microstructure.

The SEM image indicated that the TiB_2-TiC precipitates were produced in the bottom layer, and Fe_3Al-Ti_3Al was the matrix of this region (see Figure 4A). The SEM image also indicated that some of the TiB_2 precipitations were located at the grain boundaries and appeared as a small cluster (see Figure 4B). A large amount of the borons were present in the molten pool; near the interface there also existed a large amount of liquid titanium due to the dilution action, so the liquid titanium can react with boron leading to the formation of borides in the interface zone (see Figure 4C). It was also noted that the α-Ti acicular martensite was produced in the heat-affected zone, which was beneficial in improving the mechanical properties.

3.3 Micro-hardness and wear resistance

The micro-hardness as a function of depth from the top of the coating to substrate is shown in Figure 5. The micro-hardness distributions of the Fe_3Al-B_4C-YPSZ-Al_2O_3 laser clad composites exhibited clearly three steps corresponding to the upper layer, the bottom layer and the transition layer. It was noted that the micro-hardness of the upper

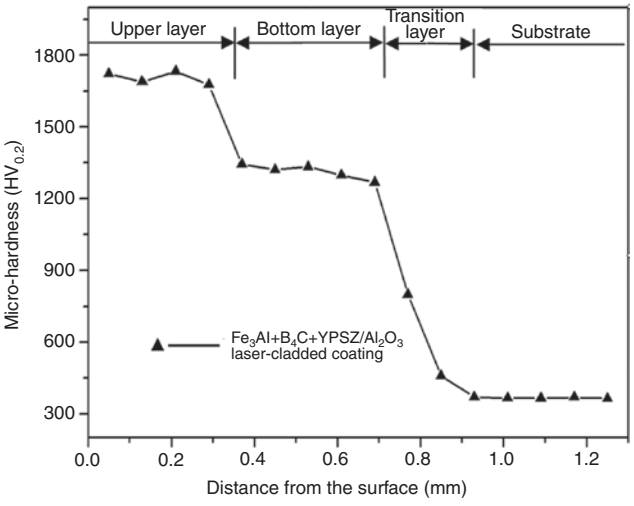

Figure 5: Micro-hardness distributions of the Fe_3Al-B_4C-YPSZ-Al_2O_3 laser clad composites.

layer was in a range of 1650~1750 $HV_{0.2}$, which was approximately 4~5 times higher compared with substrate (about 360 $HV_{0.2}$). It was considered that an enhancement of the micro-hardness of this upper layer was mainly attributed to the phase constituent. In addition, the micro-hardness distributions decreased to 1200~1350 $HV_{0.2}$ in the bottom layer. An enhancement of the micro-hardness in this region was mainly ascribed to the production of the Fe_3Al-Ti_3Al-TiB_2-TiC hard phases/the grain refinement strengthening.

The friction coefficient of such composites and Ti-3Al-2V substrate as a function of the normal load sliding against the quenching and tempering steels is shown in Figure 6. It was noticed that the friction coefficient of Ti-3Al-2V was insensitive to the normal load. Nevertheless, such composite was very sensitive to the normal load. It was clear that the friction coefficient of such composites was always lower than that of the substrate. The coefficient of such composites decreased from 0.46 to 0.37 with increase of the contact load ranging from 15 to 55 N. The friction coefficient test results indicated that such composites exhibited better wear resistance than that of the substrate under drying sliding condition [18].

When the load was 5 kg, the wear test result revealed that the wear volume loss of the Ti-3Al-2V alloy substrate was approximately 4~6 times greater than that of the composites (see Figure 7), which was mainly ascribed to the lower micro-hardness of the substrate; moreover, the wear test results also demonstrated that this coating was tightly bonded to the substrate and exhibited an effective property of the wear resistance. The wear resistance of the bottom layer is worse compared with the upper layer.

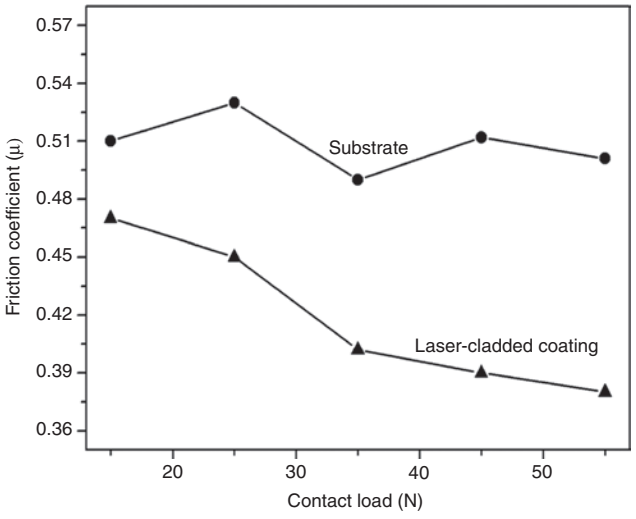

Figure 6: Variations of friction coefficients of the Fe_3Al-B_4C-YPSZ-Al_2O_3 laser clad composites and the Ti-3Al-2V substrate.

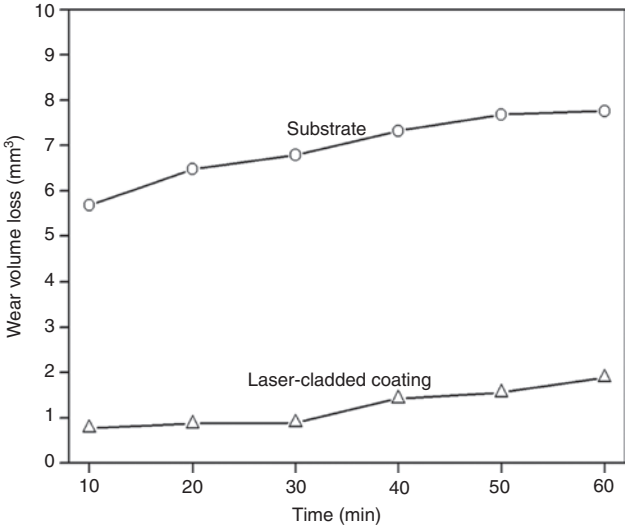

Figure 7: Wear volume losses of the Fe_3Al-B_4C-YPSZ-Al_2O_3 laser clad and the Ti-3Al-2V alloy.

Nevertheless, the bottom layer also showed better wear resistance relative to the substrate due to the actions of the hard phases and the grain refinement strengthening. In addition, the investigation [19] revealed that Al_2O_3 can further improve the hardness, elastic modulus and high temperature mechanical properties of the Al_2O_3-ZrO_2-Y_2O_3 coating. Moreover, TiO_2 is the most effective additive for improving sintering and mechanical properties [20]. Thus, it was considered that the production of Al_2O_3-TiO_2 was beneficial in improving the wear resistance of the upper layer. Furthermore, the production of Ti_3Al, TiC-Fe_3Al eutectic and TiC-Al_2O_3 also improved the wear resistance of this region. Therefore, it was reasonable that the upper layer of the composites showed an excellent wear resistance.

The SEM results revealed that the upper layer surface was smoother than that of the substrate, and the upper layer surface was characterized by the presence of few grooves and little adhesive features (see Figure 8A and B); this was proved that such composites showed better wear resistance than that of the substrate. As is shown in Figure 8C, the hard phases were present in the bottom layer, which increased the wear resistance. Nevertheless, due to the lower micro-hardness of the bottom layer, the obvious grooves were produced in the bottom layer surface after the wear test.

4 Conclusions

In summary, laser cladding of the Fe_3Al-B_4C-ZrO_2-Al_2O_3 pre-placed powders on the Ti-3Al-2V alloy can form the

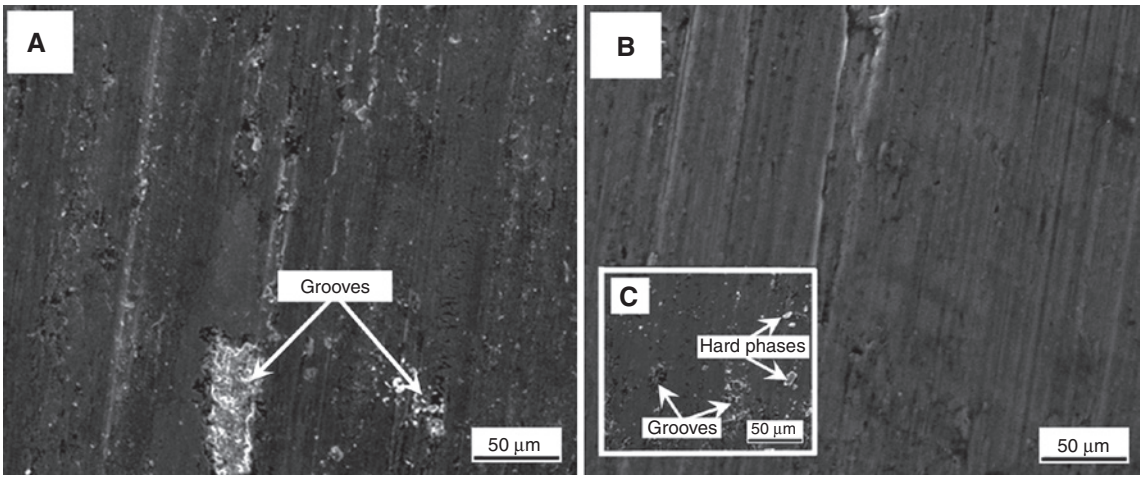

Figure 8: Worn morphologies of (A) the Ti-3Al-2V alloy, (B) the upper layer, and (C) the bottom layer of the Fe_3Al-B_4C-YPSZ-Al_2O_3 laser clad composites.

TiC-TiB_2 reinforced ceramic layer, which improved the wear resistance of the substrate. Due to the action of YPSZ, stratification was observed. There were mainly t-ZrO_2, TiO_2, TiB_2 and TiC in the precipitates of the upper layer, and the matrix of this region mainly consisted of the inter-dendritic TiC-Fe_3Al eutectic and Ti_3Al-Al_2O_3. The production of TiO_2-Al_2O_3 improved the mechanical properties of this region. Due to the action of this phase constituent, the upper layer exhibited an excellent wear resistance. The wear resistance of the bottom layer is worse compared with the upper layer. Due to the actions of the Fe_3Al-Ti_3Al-TiB_2-TiC hard phases and the grain refinement strengthening, the bottom layer also showed better wear resistance compared with the substrate.

References

[1] Gao YL, Wang CS, Pang HJ, Liu HB, Yao M. *Appl. Surf. Sci*. 2007, 253, 4917–4922.
[2] Dutta Majumdar J, Kumar A, Li L. *Tribol. Inter*. 2009, 42, 750–753.
[3] Li JN, Chen CZ, Zong L. *Int. J. Refract. Met. Hard Mater*. 2011, 29, 49–53.
[4] El-Tayeb NSM, Yap TC, Brevern PV. *Tribol. Inter*. 2010, 43, 2345–2354.
[5] Liang YH, Wang HY, Yang YF, Du YL, Jiang QC. *Int. J. Refract. Met. Hard Mater*. 2008, 26, 383–388.
[6] Jiang QC, Ma BX, Wang HY, Dong YP. *Compos. Part A: Appl. Sci. Manuf*. 2006, 37, 133–138.
[7] Ouyang JH, Nowotny S, Richter A, Beyer E. *Ceram. Inter*. 2001, 27, 15–24.
[8] Yan YY, Han Y, Huang JJ. *Scripta Mater*. 2008, 259, 203–206.
[9] Sarkar D, Adak S, Mitra NK. *Compos. Part A: Appl. Sci. Manuf*. 2007, 38, 124–131.
[10] Xue YF, Xu DP, Zhang GQ, Zhou XF, Ding ZH, Li XM, Su WH. *Chem. Res. Chinese U.* 2008, 24, 135–137.
[11] Ouyang JH, Nowotny S, Richter A, Beyer E. *Surf. Coat. Technol*. 2001, 137, 12–20.
[12] Ma WM, Lei W, Guan RG, Sun XD, Li XK. *Mater. Sci. Eng. A* 2008, 477, 100–106.
[13] Du BS, Paital SR, Dahotre NB. *Scripta Mater*. 2008, 59, 147–150.
[14] Vasiliev LA, Padture NP. *Acta Mater*. 2006, 54, 4921–4928.
[15] Jackson KA. *Mater. Sci. Eng*. 1984, 65, 7–13.
[16] French JD, Harmer MP, Chan HM, Miller GA. *J. Am. Ceram. Soc*. 1990, 73, 2508–2510.
[17] Wang CL, Wang MX, Yu BH, Chen D, Qin P, Feng MH, Dai QR. *Mater. Sci. Eng. A* 2007, 459, 238–243.
[18] Li JN, Chen CZ, Hu JH. *Surf. Interface Anal*. 2012, 44, 559–564.
[19] Zhang YS, Chen JM, Hu LT, Liu WM. *Mater. Lett*. 2006, 60, 2302–2305.
[20] Van Acker K, Vercammen K. *Wear* 2006, 256, 353–361.